Available online at www.sciencedirect.com
SCIENCE DIRECT
Comparative Biochemistry and Physiology, Part B 144 (2006) 510–519
CBP
www.elsevier.com/locate/cbpb

Neuronal nitric oxide synthase in the gill of the killifish, *Fundulus heteroclitus*

Kelly A. Hyndman [a,b,*], Keith P. Choe [b,c], Justin C. Havird [a,b], Rachel E. Rose [a,b], Peter M. Piermarini [d], David H. Evans [a,b]

[a] *Department of Zoology, University of Florida, Gainesville, FL 32611, USA*
[b] *Mount Desert Island Biological Laboratory, Salisbury Cove, ME 04672, USA*
[c] *Anesthesiology Research Division, Vanderbilt University Medical Center, Nashville, TN 37232, USA*
[d] *Department of Cellular and Molecular Physiology, Yale University School of Medicine, New Haven, CT 06520, USA*

Received 23 January 2006; received in revised form 3 May 2006; accepted 12 May 2006
Available online 19 May 2006

Abstract

Neuronal NOS (nNOS) is a constitutively expressed enzyme that catalyzes the oxidation of L-arginine and water to L-citrulline and the gas nitric oxide (NO). Nitric oxide is involved in regulation of a variety of processes, including: vascular tone, neurotransmission, and ion balance in mammals and fishes. In this study, we have cloned and characterized a putative NOS homologue from the brain of the euryhaline killifish, *Fundulus heteroclitus*. Killifish NOS has 75% amino acid identity to human nNOS, and phylogenetic analysis groups the killifish sequence with the mammalian nNOS, suggesting that it is a mammalian orthologue. Relative quantitative reverse transcriptase-PCR demonstrated that killifish nNOS mRNA is highly expressed in the brain and gill followed by the stomach, kidney, opercular epithelium, intestine and heart. Immunohistochemistry localized nNOS to nerve fibers and epithelial cells adjacent to mitochondrion-rich cells (ion transporting cell) in the gill, suggesting that nNOS production of NO may contribute to regulation of vascular tone and/or MRC function in the teleost gill.

Keywords: *Fundulus heteroclitus*; Gill; Killifish; Neuronal nitric oxide; Ion transport; Nerve; Vascular tone; Mitochondrion-rich cell

1. Introduction

The gas nitric oxide (NO) is the endothelium derived relaxing factor in mammals (Ignarro et al., 1987; Palmer et al., 1987), and it functions in a variety of physiological processes such as regulation of vascular tone, platelet aggregation and adhesion, neurotransmission, cell growth, and apoptosis (Blaise et al., 2005). Nitric oxide is produced in the body by the oxidation of L-arginine and water to L-citrulline and NO by nitric oxide synthases (NOS). In mammals, there are three NOS isoforms transcribed from separate genes, endothelial NOS (eNOS or NOS3) and neuronal NOS (nNOS or NOS1) that are constitutively expressed, and inducible NOS (iNOS or NOS2). In fishes, there appears to be only two NOS genes: nNOS and iNOS (Oyan et al., 2000). In GenBank, cDNA sequences for nNOS and iNOS from fishes are available (see Fig. 3 caption for accession numbers), and searching of the completed fish genome projects reveals only nNOS and iNOS sequences. Thus, there are currently no molecular data to support the existence of eNOS in this group of vertebrates, suggesting that nNOS may be the only constitutively expressed NOS isoform. In addition, physiological studies have suggested that prostaglandins, not NO, are the endothelial-derived relaxing factors in fishes (Olson and Villa, 1991; Farrell and Johansen, 1995; Evans and Gunderson, 1998), which also supports the hypothesis that eNOS is not found in this group. Nevertheless, heterologous antibodies have been used to detect eNOS-like immunoreactivity in fishes such as the zebrafish (*Danio rerio*) (Fritsche et al., 2000), tilapia (*Oreochromis niloticus*) (Cioni et al., 2002), and Atlantic salmon (*Salmo salar*) (Ebbesson et al., 2005). Recently, Tota et al. (2005)

* Corresponding author. Department of Zoology, University of Florida, Bartram 231, P.O. Box 118525, Gainesville, FL 32611, USA. Tel.: +1 352 392 1489; fax: +1 352 392 3704.
E-mail address: khyndman@zoo.ufl.edu (K.A. Hyndman).

1096-4959/$ - see front matter © 2006 Elsevier Inc. All rights reserved.
doi:10.1016/j.cbpb.2006.05.002

reported eNOS-like immunoreactivity in hearts from the teleosts: *Anguilla anguilla*, *C. hamatus*, *Protopterus dolloi*, *Thunnus thynnus thynnus*, and *Trematomus bernacchii*.

Although, it appears endothelial cells do not produce NO in fishes, NO is hypothesized to function in regulation of vascular tone. Olson and Villa (1991) determined that trout vessels lack a non-prostanoid endothelial-derived relaxing factor, but that they do contain the NO receptor, soluble guanylyl cyclase. As well, numerous studies have demonstrated that teleost vessels are dilated by nitric oxide donors (Soderstrom et al., 1995; McGeer and Eddy, 1996; Olson et al., 1997; Evans and Harrie, 2001), suggesting that NO is a regulator of vascular tone. Recently, Jennings et al. (2004) demonstrated that the eel (*Anguilla australis*) dorsal aorta and intestinal veins are innervated with nNOS-positive nerves, and that NO released from these nitrergic fibers regulated smooth muscle vascular tone. In addition, nitrergic fibers also have been localized in the fish brain (Mauceri et al., 1999; Holmqvist et al., 2000; Oyan et al., 2000; Cuoghi et al., 2002; Bordieri et al., 2003; Ando et al., 2004), and gill (Mauceri et al., 1999; Zaccone et al., 2003; Ebbesson et al., 2005). The gill also contains nNOS-positive neuroendocrine cells (Mauceri et al., 1999; Zaccone et al., 2003; Ebbesson et al., 2005). Since the fish gill is a highly vascularized tissue that functions in gas exchange, acid–base regulation, nitrogen excretion and osmotic and ion regulation we have hypothesized that NO released from these nitrergic fibers may play an important role in controlling gill function (Evans et al., 2005).

Nitric oxide has also been shown to affect ionic transport across various epithelial tissues (Tipsmark and Madsen, 2003; Evans et al., 2004; Ebbesson et al., 2005), and our recent work has demonstrated that NO donors can inhibit ion transport across the fish gill epithelium (Evans et al., 2004). The gill of seawater (SW) teleosts contains ion regulating cells, termed mitochondrion-rich cells (MRCs) that are also rich in Na^+, K^+,-ATPase (NKA) (Karnaky et al., 1976; Katoh et al., 2001), the enzyme responsible for maintaining the electrochemical gradient to drive NaCl transport. The NO-donor sodium nitroprusside (SNP) has been shown to inhibit NKA activity in salmonid gill (Tipsmark and Madsen, 2003; Ebbesson et al., 2005). These studies suggest that NO may be a regulator of MRC-mediated, gill ion transport, as well a gill perfusion, in fishes.

The killifish is a euryhaline teleost that is a model organism for fish osmoregulation (e.g. Karnaky and Kinter, 1977; Marshall et al., 1999; Hoffmann et al., 2002; Evans et al., 2004). This fish can survive direct transfer from freshwater to full strength seawater (32 ppt) making it an ideal organism to examine rapid regulation of ion transport. The purposes of this study were to determine the mRNA sequence of nNOS from the euryhaline teleost, *Fundulus heteroclitus*, examine the tissue distribution of the nNOS mRNA, and determine which cells in the gill express the nNOS protein.

2. Materials and methods

2.1. Animal collection

Killifish, *F. heteroclitus*, were caught in the brackish waters of Northeast Creek, Salisbury Cove, Maine. They were maintained in free flowing seawater (SW), for a minimum of a week, before being shipped to the University of Florida were they were maintained in full-strength SW (32 ppt) at 24±1 °C for over 30 days. The holding tanks were maintained at a pH between 7.8 and 8.2, and ammonia, nitrate, and nitrite levels were below 1 ppm.

2.2. Reverse transcriptase-polymerase chain reaction (RT-PCR), cloning, and sequencing

Molecular protocols similar to those of Choe et al. (2005) were used. In short, killifish were decapitated, and the brain was removed with sterile, RNAse-free tools, and frozen in liquid nitrogen. The brain was the tissue expected to have the highest level of nNOS, thus to determine the killifish nNOS sequence the brain was used. Total RNA was then isolated with TRI-reagent (Sigma-Aldrich, St. Louis, MO, USA), and first-strand cDNA was synthesized from 2 μg of total RNA with a Superscript™ II reverse transcriptase kit (Invitrogen, Carlsbad, CA, USA) using oligo-dT as a primer. Degenerate primers were designed using CODEHOP (Rose et al., 2003): nNOS F1 5′ *CCA CCC TAA GTT CGA TGG TTY AAR GA* 3′ and nNOS R1 5′ *GAC ATA GGA GGC ACG ATC CAN ACC CA* 3′, and used for initial cloning and sequencing of the killifish brain nNOS. Each PCR was performed on 1/20th of a reverse transcriptase reaction with a FastStart Taq DNA Polymerase kit (Roche Applied Science, Indianapolis, IN, USA) in a PCR Express thermocycler (ThermoHybaid, Franklin, MA, USA) with standard cycling parameters. PCR products were visualized by ethidium bromide staining in 1.0% to 1.5% agarose gels, ligated into pCR®4-TOPO vectors, and transformed into TOP10 chemically competent cells using a TOPO TA Cloning® Kit for sequencing (Invitrogen). Plasmid DNA was then sequenced in both directions at the Marine DNA Sequencing Facility at the Mount Desert Island Biological Laboratory (Salisbury Cove, ME). After the sequencing of the initial fragment, more of the cDNA for nNOS was cloned and sequenced using a combination of degenerate and non-degenerate primers, and by 5′ and 3′ rapid amplification of cDNA ends (5′ and 3′ RACE). 5′ and 3′ RACE cDNA was prepared with a GeneRacer™ Kit (Invitrogen) according to the manufacturer's protocols. PCR, cloning, and sequencing were performed as above.

2.3. Sequence and phylogenetic analysis

Sequence results for each initial degenerate primer pair were assembled and the resulting amino acid translations were analyzed with the basic local alignment search tool (Blast) on the National Center for Biotechnology Information website. Killifish nNOS fragment sequences were assembled with GeneTools software (BioTools Inc., Edmonton, AB, Canada) and the assembled nucleotide sequence was searched for open reading frames. The predicted amino acid sequence was aligned with other full-length vertebrate nNOS proteins using Clustal X (Chenna et al., 2003). The expected locations of enzymatic activity and regions important for regulation of the enzyme were taken from previously published reports (Crane et al., 1997; Alderton et al., 2001; Zhang et al., 2001; Garcin et al., 2004) and from the Ensembl Human database (ENSP00000337459). The alignment was exported to PHYML (Guindon et al., 2005) and a Fast

Maximum-Likelihood test was performed, following the WAG model of amino acid substitutions and a gamma calculated of 1.363. Branches were then tested for statistical significance by bootstrapping with 500 replicates. The bootstrap trees were then imported to PHYLIP (Felsenstein, 2004) and a consensus tree was constructed. All sequences were taken from GenBank except the NOS sequence from *Ciona intestinalis*, which was derived from the *Ciona* genome database.

2.4. Multiple tissue relative quantitative PCR

To determine the distribution of nNOS mRNA among tissues, relative quantitative RT-PCR was performed on total RNA from gill, opercular membrane, brain, heart, stomach, intestine, and kidney tissue as described previously (Choe et al., 2004, 2005). Briefly, cDNA was produced from the tissues of a SW killifish as described above, but random hexamer primers (not oligo-dT primers) were used so that ribosomal and messenger RNA would be reverse transcribed. Non-degenerate primer pairs: nNOS DF1 5′*GGA GAC TGG GTG TGG ATT GTG* 3′, and nNOS DR1 5′ *CCG TTG CCA AAT GTA CTG* 3′, were designed to amplify a product with high efficiency (e.g., high melting temperature). To minimize the chance of amplifying contaminating genomic DNA, the primer pair was designed to include at least one intron–exon boundary that is conserved between vertebrate NOS homologues. A QuantumRNA™ 18S internal standard primer kit (Ambion, Woodward Austin, TX) was used to control for variability in RNA quality and quantity between the different tissues tested. Multiplex PCR with primers for 18S and nNOS were then optimized to ensure that the reactions were terminated during the exponential phase and that the kinetics of 18S amplification approximated those of nNOS. Lastly, the products were visualized by ethidium bromide staining in 1.5% agarose gels and photographed with Polaroid 667 film. The Polaroid was then digitized by scanning it with a flatbed scanner.

2.5. Tissue collection for immunohistochemistry

Five killifish were sacrificed and the second gill arch from the right side was excised. These gills were fixed for 1 h in 3% paraformaldehyde/0.05% picric acid/0.05% glutaraldehyde fixative in 10 mM phosphate-buffered saline (PBS), at 4 °C followed by three 15 min washes in 10 mM PBS. The tissues were then kept in 75% ethanol until embedding. To prepare for the paraffin embedding, the tissues were dehydrated through an increasing concentration of ethanol (75% to 100%), cleared for 2 h in Citrosolv (Fisher Scientific, Pittsburgh, PA, USA), and embedded in paraffin wax. Tissue sections were then cut 5 μm thick perpendicular to the lamellae to allow visualization of intralemallar and interlamellar regions. Tissue sections were placed on Super-frosted positive charged slides (Fisher Scientific) and dried overnight at 30 °C.

2.6. Immunohistochemistry

>We followed the immunohistochemical methods of Piermarini et al. (2002). In short, the gill sections were deparaffinized in Citrisolv and rehydrated in a decreasing ethanol series (100% to 35%) followed by 10 mM PBS. The tissue sections were circled with a PAP-Pen (Electron Microscopy Sciences, Hatfield, PA, USA) to create a hydrophobic barrier and incubated with a 200 μL of 3% H_2O_2 (diluted in water) for 30 min at room temperature (~24 °C) to block endogenous peroxidases. The slides were then blocked with Biogenex's protein block (BPB, normal goat serum with 1% bovine serum albumin, 0.09% NaN_3, and 0.1% Tween 20) (Biogenex, San Ramon, CA, USA) at room temperature for 20 min. Sections were then rinsed with 10 mM PBS and incubated overnight with anti-nNOS (1/500, see below) at 4 °C. After a 5 min wash in 10 mM PBS, the slides were subjected to the horse-radish peroxidase, Super Sensitive™ Link-Label IHC Detection System (Biogenex). Briefly, slides were incubated in a humidified chambered at 25 °C for 20 min with 10 μL of "Label" (biotinylated anti-immunoglobulins) per tissue section, followed by a 5 min PBS wash and a 20 min incubation with "Link" (peroxidase-conjugated streptavidin). Finally, antibody binding was visualized by applying 3, 3′-diaminobenzidine tetrahydrochloride (DAB) (brown color, Biogenex) for 5 min at room temperature. Excess DAB was removed by rinsing the slides for 5 min under running tap water. Double-labeled slides were then incubated with BPB again and anti-NKA (1/1000, see below) overnight at 4 °C. Following a 5 min wash in 10 mM PBS, the sections were incubated with the Link and Label as described above. Visualization of the second antibody was accomplished with Vector SG (blue color, Vector Laboratories, Burlingame, CA, USA). The slides were then dehydrated through an increasing ethanol concentration series, and mounted in Permount (Fisher Scientific). Negative controls were generated by following the above methods except that BPB was used instead of the primary antibody.

2.7. Antibodies

Neuronal NOS (nNOS) was localized with a commercial affinity purified polyclonal antibody made against amino acids 724 to 739 of human nNOS (Chemicon International, Inc., Temecula, CA, USA). Monoclonal, anti-NKA (α5) was developed by Dr. Douglas Fambrough, and was obtained from the

Fig. 1. nNOS alignment of the oxygenase region and calmodulin binding domains. Similar amino acids are shaded grey. All domains are based upon published crystallography studies completed with *Rattus* nNOS (McMillan and Masters, 1995; Crane et al., 1997). *Fundulus* Cys^{406} aligns with Cys^{415} in the *Rattus* (yellow highlight) and is believed to function in heme binding (Masters et al., 1996). The antigen used to make the nNOS antibody is highlighted in yellow in the calmodulin binding domain and shows that *Fundulus* nNOS has 15/16 amino acids in common with the antigen. Accession numbers: *Rattus norvegicus* P29476, *Homo sapiens* NP 000611, *Gallus gallus* NP 990292, *Xenopus laevis* AAD55136, *Oryzias latipes* BAD11808, *Fundulus heteroclitus* AY533030, *Danio rerio* NP 571735, *Takifugu poecilonotus* AAM46138. *Marks every 10 amino acids.

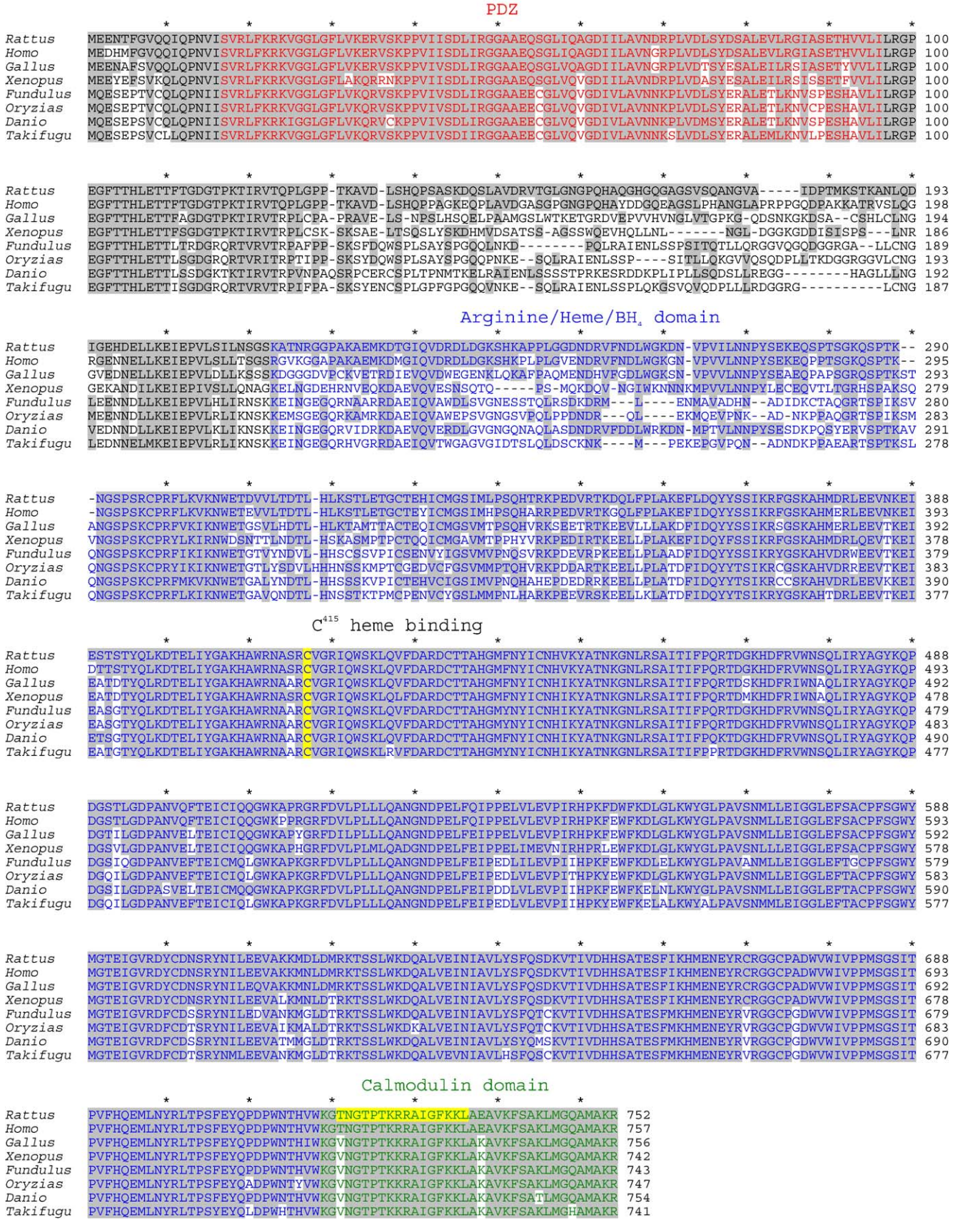
PDZ
Arginine/Heme/BH4 domain
C415 heme binding
Calmodulin domain
Rattus
Homo
Gallus
Xenopus
Fundulus
Oryzias
Danio
Takifugu

Developmental Studies Hybridoma Bank, which was developed under the auspices of the National Institute of Child Health and Human Development of the University of Iowa, Department of Biological Sciences, Iowa City, IA, USA. All antibodies were diluted in BPB.

2.8. Western blot analysis

Western blot analysis was performed as previously published by Piermarini et al. (2002). Five killifish were sacrificed and the gills excised to generate 0.8 g of tissue,

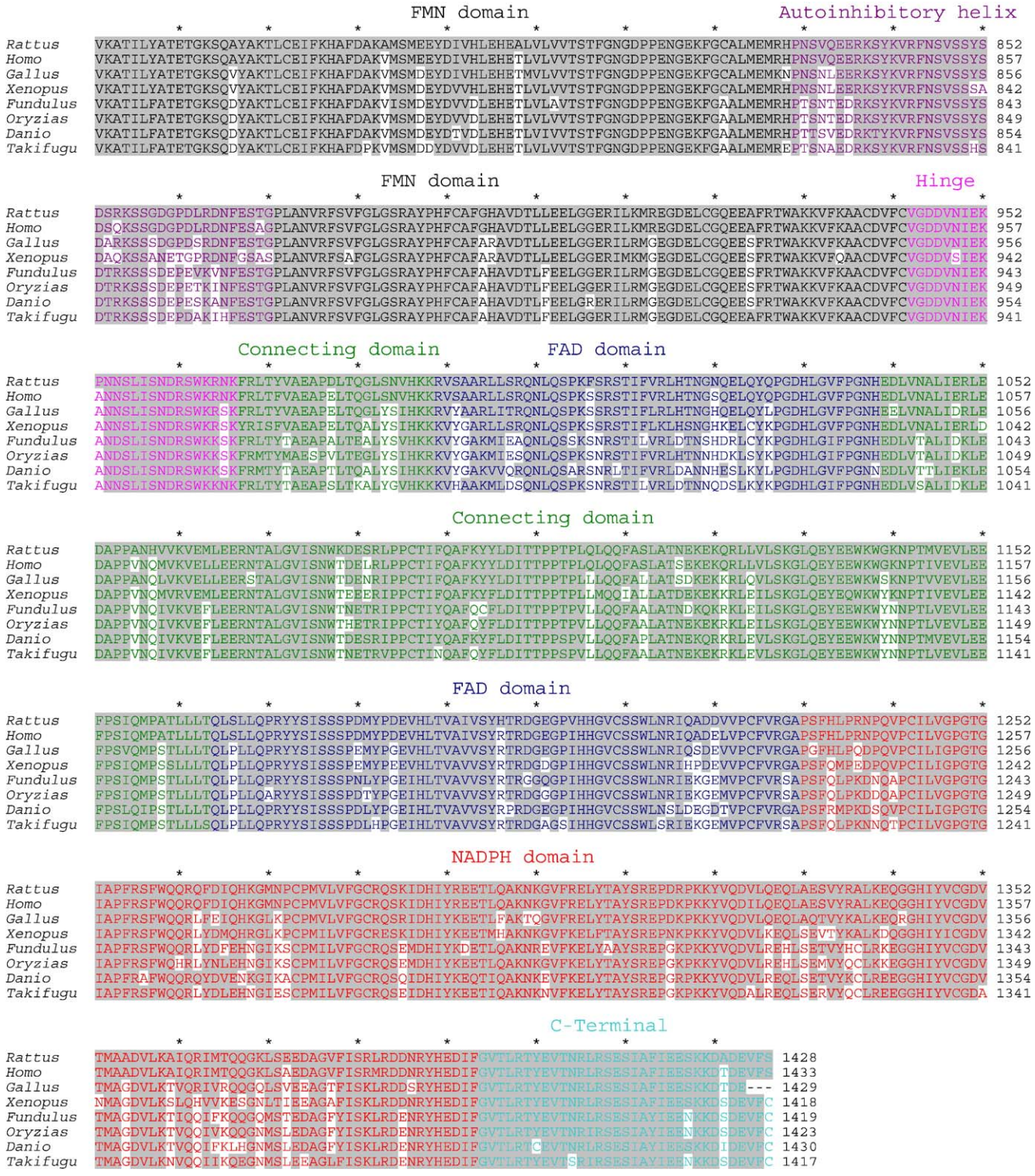

Fig. 2. nNOS alignment of the reductase region. Similar amino acids are shaded in grey. All domains are predicted from published crystallography studies with *Rattus* nNOS (McMillan and Masters, 1995; Crane et al., 1997; Garcin et al., 2004). These domains include: FMN (black), FAD (blue) and NADP (red) binding domains. See Fig. 1 for accession numbers.

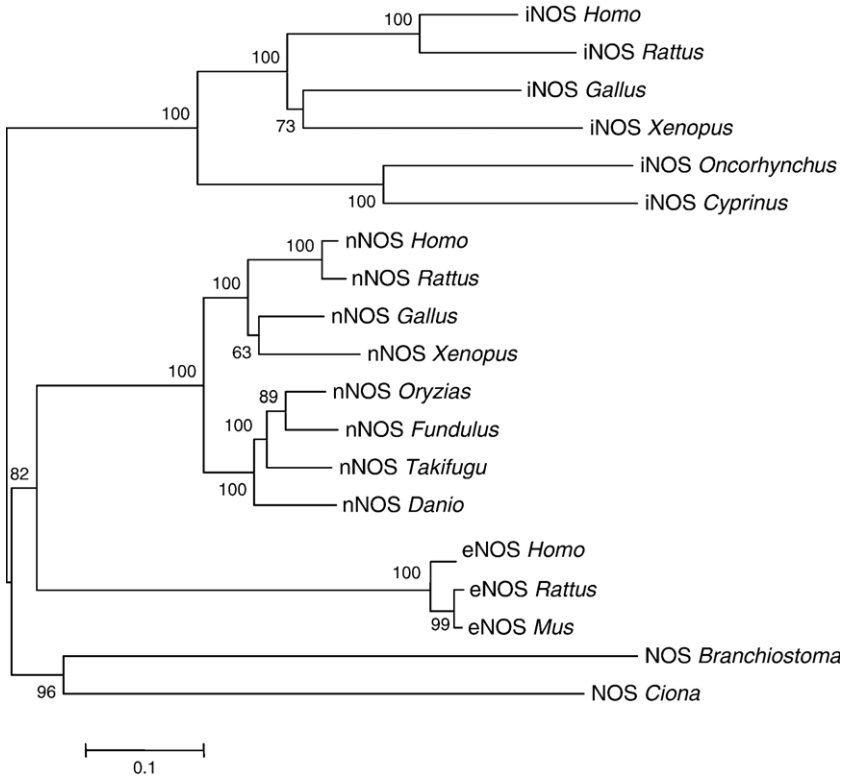

Fig. 3. An unrooted phylogenetic tree displaying the relationship between the NOS family of enzymes. Using PHYML, a maximum-likelihood test with WAG estimation of amino acid substitutions and a gamma of 1.363 was used to determine the relationship between the chordate NOS genes (Guindon et al., 2005). To test the strength of the branch lengths, a bootstrap of 500 replicates was also run and the numbers at the nodes represent the percent bootstrap number as determined by PHYLIP (Felsenstein, 2004). Accession numbers from top to bottom: *Homo sapiens* iNOS NP 000616, *Rattus norvegicus* iNOS NP 036743, *Gallus gallus* iNOS NP 990292, *Xenopus tropicalis* iNOS scaffold_456: 754,909–778,335, *Oncorhynchus mykiss* iNOS CAC82807, *Cyprinus carpio* iNOS CAB60197, *H. sapiens* nNOS NP 000611, *R. norvegicus* nNOS P29476, *G. gallus* nNOS NP 990292, *Xenopus laevis* nNOS AAD55136, *Oryzias latipes* nNOS BAD11808, *Fundulus heteroclitus* nNOS AY533030, *Takifugu poecilonotus* nNOS AAM46138, *Danio rerio* nNOS NP 571735, *R. norvegicus* eNOS NP_068610, *Mus musculus* eNOS NP 032739, *H. sapiens* eNOS NP 000594, *Branchiostoma floridae* NOS AAQ02989, *Ciona intestinalis* NOS Scaffold_674: 1547–25147.

which was homogenized in ice-cold homogenization buffer (250 mM sucrose, 30 mM Tris, 1 mM EDTA, 2 μg mL^{-1} leupeptin, and 100 μg mL^{-1} phenylmethylsulfonyl fluoride; pH 7.8). The homogenate was centrifuged at 300×*g* for 5 min to remove cell debris. The supernatant was then centrifuged at 10,000×*g* for 10 min to remove mitochondria; this resulting supernatant was further centrifuged at 100,000×*g* for 90 min to pellet microsomes. All centrifugation steps were performed at 4 °C. The microsomal pellet was resuspended in homogenization buffer and then diluted 1/2 in 2× Laemmli sample buffer (Laemmli, 1970) without bromophenol blue and β-mercaptoethanol. The supernatant was also diluted 1/2 with the 2× Laemmli sample buffer. Protein content of the resuspended pellet and supernatant was determined using a BCA detergent compatible protein assay kit (Pierce, Rockford, IL, USA). Next, 2% β-mercaptoethanol and 0.01% Bromophenol Blue were added to each sample and they were heated at 65 °C for 10 min. Twenty-five micrograms of total protein from each sample was then separated in SDS-PAGE, 7.5% Tris–HCl precast polyacrylamide gels (Bio-Rad, Hercules, CA, USA) for 2 h at 100 V and then transferred to an Immuno-blot PVDF membrane (BioRad) according to the manufacturer's protocol. Membranes were then rehydrated in 100% methanol for 5 min followed by two water rinses. They were then placed in Blotto, 5% non-fat dry milk in TBS (25 mmol L^{-1} Tris, 150 mmol L^{-1} NaCl; pH 7.4) at room temperature for 1 h while shaking. Membranes were then incubated with 1/500 nNOS overnight at

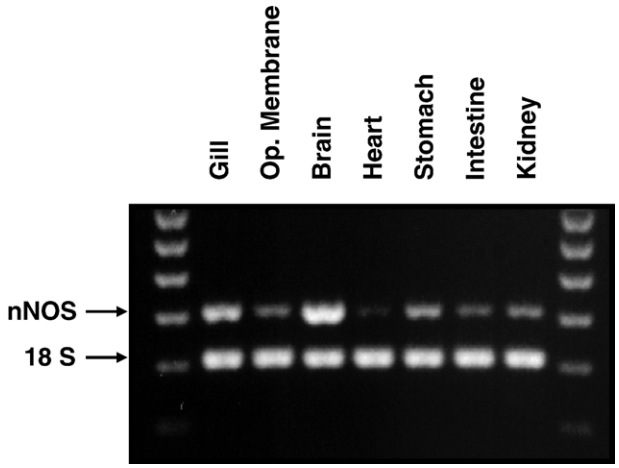

Fig. 4. Tissue distribution of the killifish nNOS expression. Non-degenerate primers were used to amplify a 415 bp product (upper band) from cDNA made from gill, operculum membrane (epithelium), brain, heart, stomach, intestine, and kidney RNA. The lower band is the internal control (18S) that amplified a 315 bp product (lower band).

4 °C, while shaking. After three washes with TTBS (0.1% Tween-20 in TBS; pH 7.4), the membrane was incubated with alkaline-phosphatase-conjugated goat anti-rabbit IgG (1/3000 diluted in Blotto) for 1 h at room temperature. Antibody binding was detected by exposing Amersham-Pharmacia's Hyperfilm (Piscataway, NJ, USA) to a chemiluminescent signal (Immun-star chemiluminescent kit, BioRad) according to the manufacturer's protocol. All proteins on the membrane were exposed by incubating the membrane in 0.02% Coomassie blue/50% methanol/10% acetic acid/40% water for 1 min. Negatives and the Coomassie blue stained membrane were digitized using a flatbed scanner and adjusted for brightness and contrast with Adobe Photoshop CS 8.0 (San Jose, CA, USA).

3. Results

3.1. Molecular identification of nNOS

The completed putative killifish nNOS (Accession: AY533030) contains 4590 nucleotides with a predicted open reading frame of 4260 nucleotides that translates into a 1420 amino acid protein (Figs. 1 and 2). The likely start codon (AUG) is 218 nucleotides downstream of the 5′ end of the cDNA obtained by RACE. The stop codon (UAG) is 87 nucleotides up stream from the start of the 3′ poly A tail.

nNOS appears to be highly conserved throughout the vertebrates, and the killifish nNOS sequence includes a putative PDZ domain, the Cys^{406} (Cys^{415} in rats and Cys^{420} in humans)

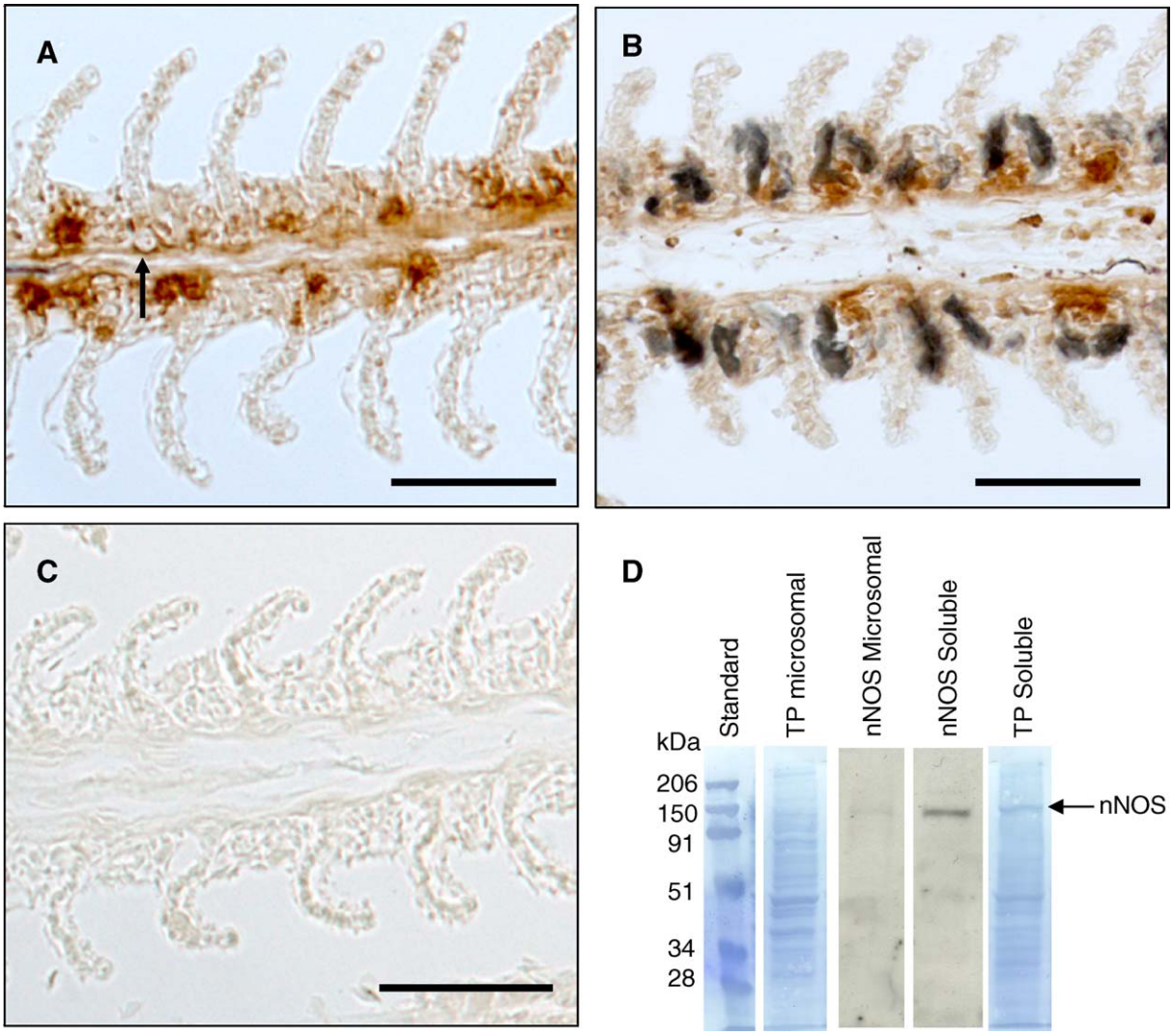

Fig. 5. Representative light micrographs of killifish gill sections incubated with nNOS antibody (A and B) or Biogenex's protein block (BPB) (C), and binding of nNOS antibody on a Western blot (D). (A) nNOS-immunoreactivity (nNOS-IR, visualized with diaminobenzidine tetrahydrochloride, brown) was observed in epithelial cells of the interlamellar region of the filament, and in hypothesized nerve fibers that run along the interlamellar vessels and lamellar arterioles (arrow). (B) Double labeling the gill with anti-nNOS (brown) and anti-NKA (visualized with Vector SG, blue) demonstrates that the nNOS-IR epithelial cells are adjacent to the NKA-IR cells. (C) No immunoreactivity was seen in the negative control sections incubated with BPB instead of the nNOS antibody. Scale bar = 50 μm. (D) The nNOS antibody binds to a protein in the soluble fraction (nNOS soluble) of the Western blot, with a molecular weight of ~150 kDa. This band is also seen in the total protein (TP) soluble fraction of the coomassie blue stained membrane. A faint band was also detected in the microsomal fraction (nNOS microsomal). The approximate molecular masses are shown beside the standard.

(McMillan and Masters, 1995; Crane et al., 1997) heme binding nucleotide in the oxygenase region of the protein , calmodulin binding domain (Fig. 1), and FMN, FAD, and NADPH binding domains in the reductase region of the protein (Fig. 2). The antigen used to generate the nNOS antibody used in our immunohistochemistry was well conserved with the killifish nNOS (15/16 identical amino acids) and was from the calmodulin binding domain (Fig. 1). The killifish nNOS groups with the other vertebrate nNOSs in phylogenetic analysis (bootstrap 100%, Fig. 3).

3.2. Tissue distribution

Multiplex RT-PCR with cDNA from gill, opercular membrane, brain, heart, stomach, intestine, and kidney was conducted to determine the distribution of nNOS (Fig. 4). After 30 cycles of PCR with non-degenerate killifish nNOS primers, the expected 415 bp product was the most abundant in brain, followed by gill, stomach, kidney, opercular membrane, intestine, and heart. As seen in Fig. 4, the 18S primers amplified a product of the expected 315 bp size from all tissues, at relatively equal levels.

3.3. Immunolocalization and western blotting of nNOS

Neuronal nitric oxide synthase immunoreactivity (nNOS-IR) was found in epithelial cells in the interlamellar region of the gill filament (Fig. 5A and B) but was not observed in cells of the lamellae. The nNOS-IR epithelial cells were seen along the length of the filament, predominantly by the afferent filamental artery and interlamellar vessels (Fig. 5B). nNOS-IR also appeared to be in nerve fibers that run near the efferent filamental arteries (not shown), interlamellar vessels, and the lamellar arterioles (Fig. 5A arrow). Na^+, K^+,-ATPase immunoreactivity (NKA-IR) was seen in epithelial cells of the interlamellar region, near the afferent filament artery and interlamellar vessels (Fig. 5B). This localization is consistent with previous studies that used NKA antibodies to immunolocalize MRCs (Katoh et al., 2001, 2003). NKA-IR epithelial cells (MRCs) were found adjacent to the nNOS-IR cells (Fig. 5B); the NKA-IR and nNOS-IR were not in the same cell (Fig. 5B). In the absence of primary antibody, no staining was seen (Fig. 5C). The anti-nNOS labeled a single band, in the soluble fraction of the killifish gill homogenates, with a molecular weight of ~150 kDa (nNOS soluble, Fig. 5D). A faint band was also seen in the microsomal fraction of the gill homogenates (nNOS microsomal, Fig. 5D). Total protein from the microsomal and soluble lanes was stained with Coomassie blue and is shown in Fig. 5D.

4. Discussion

4.1. Molecular identification of the killifish nNOS

Our study is the first to sequence a putative nNOS from a euryhaline teleost. This nNOS contains all of the major domains found in rat NOS (Crane et al., 1997; Zhang et al., 2001; Garcin et al., 2004). These include: (1) the L-arginine, heme, and tetrahydrobiopterin (HB_4) binding domains, (2) the cysteine^{406} residue (C^{415} in rat) necessary for heme binding in the oxygenase region of the protein (McMillan and Masters, 1995; Crane et al., 1997), (3) the calmodulin binding domain, and (4) the FMN, FAD, and NADPH binding domains of the reductase region. Mammalian nNOS also contains a unique 5′ PDZ domain believed to function in anchoring of the protein to specific intracellular locations (Daff, 2003), and our killifish nNOS sequence contains this putative domain. The killifish nNOS also contains a putative autoinhibitory loop between the two FMN binding domains that in mammalian nNOS and eNOS (not found in iNOS) can inhibit FMN to heme electron transfer (Daff, 2003). Our phylogenetic analysis suggests that the killifish NOS we have sequenced is an orthologue of the mammalian nNOS (Fig. 3). The killifish nNOS groups with other teleost nNOS sequences and does not group with the teleost iNOS. Interestingly, NOS sequences from the tunicate (*C. intestinalis*) (Scaffold_674: 1547–25147) and lancelet (*Branchiostoma floridae*) (Accession: AAQ02989) group outside of vertebrate nNOS, iNOS, and eNOS, suggesting that gene duplications of NOS occurred after the tunicates diverged from the vertebrate lineage. To estimate at which point in vertebrate evolution these NOS gene duplications occurred, NOS sequences are needed from ancestral craniates like the hagfish (*Myxine glutinosa*) and lamprey (*Petromyzon marinus*).

4.2. Tissue distribution of the killifish nNOS

The killifish brain had the highest relative expression of nNOS. This is consistent with earlier observations of nNOS mRNA localization in the zebrafish brain, and suggests that nNOS plays a role in neurotransmission in fishes (Holmqvist et al., 2000). In addition, expression of nNOS in the gill, opercular membrane, and kidney suggests that the enzyme may regulate systemic ion transport. Previous studies demonstrated that nitric oxide donors inhibit NKA activity in the trout (*Oncorhynchus mykiss*) gill (Tipsmark and Madsen, 2003), salmon gill (Ebbesson et al., 2005), and trout kidney (Tipsmark and Madsen, 2003), and electrophysiological studies demonstrated that NO donors reduce short circuit current in isolated killifish opercular epithelia, indicating that net chloride transport is inhibited by NO (Evans et al., 2004).

4.3. Immunolocalization of nNOS in the killifish gill

Our immunolocalization of nNOS in epithelial cells of the killifish gill corroborates previous findings of nNOS positive cells in the interlamellar region of the teleost gill (Zaccone et al., 2003; Ebbesson et al., 2005). However, we did not find NOS-IR cells on the lamellae of the SW killifish gill, which is contrary to findings by two studies using FW catfish (*Heteropneustes fossilis*) (Zaccone et al., 2003) and FW Atlantic salmon (Ebbesson et al., 2005). This suggests that the location of cells expressing nNOS may differ among species and/or salinities. Ebbesson et al. (2005) also reported that nNOS protein and NKA mRNA colocalized to the same gill epithelial cells, but our study localized nNOS to epithelial cells that are

adjacent to the NKA-IR cells. Ebbesson et al. (2005) did not describe the antigen for their antibody, and they did not publish any controls (i.e. Western blots or preabsorption of antibody with antigen), so it is unclear whether their antibody cross-reacted with iNOS or is binding non-specifically. The epitope for our nNOS antibody is 93% homologous with the killifish nNOS sequence but only 19% homologous with iNOS from the common carp (*Cyprinus carpio*) (accession AJ242906.1), and 25% homologous with iNOS from the trout (accession AJ295230.1), suggesting that our antibody is specific for nNOS. In addition, our nNOS antibody recognized a single protein of 150 kDa, which corroborates a previous study that immunoblotted nNOS from the tilapia spinal cord (Cioni et al., 2002). Our observation of nNOS expression in cells adjacent to MRCs in killifish gill suggests that NO may be acting as a paracrine signaling molecule to regulate systemic NaCl secretion. The exact cellular targets and effects of NO in MRCs are unknown, but may include inhibition of NKA and net NaCl secretion (Tipsmark and Madsen, 2003; Evans et al., 2004).

Nitric oxide synthase immunoreactivity was previously observed in structures that were hypothesized to be nerve fibers in the gill the of catfish (Mauceri et al., 1999; Zaccone et al., 2003), and NADPH-diaphorase activity (an indicator of NOS protein) was observed in hypothesized nerve fibers in the gill of the cod (*Gadus morhua*) (Gibbins et al., 1995). Recently, extensive innervation of the zebrafish gill was demonstrated by staining for multiple neuronal markers (zebrafish specific neuron marker Zn-12, serotonin, synaptic vesicle protein SV2, and a purinoceptor expressed in sensory Rohon-Beard cells of the zebrafish) (Jonz and Nurse, 2003). In a pufferfish (*Takifugu niphobles*), nitrergic innervation of the gill was demonstrated by nNOS immunoreactivity and NADPH diaphorase activity in the glossopharyngeal and vagal sensory ganglia (originating from the medulla oblongata) that terminate by the efferent filamental arteries of the gill (Funakoshi et al., 1999). It was hypothesized that these sensory nitrergic fibers function in regulation of the baroreceptor reflex in fishes (Funakoshi et al., 1999). Our immunolocalization of nNOS in fibers running along the vasculature is consistent with the innervation reported for zebrafish and pufferfish, suggesting that NO may be involved in neurotransmission and/or the baroreceptor reflex in the killifish gill. In addition, these nitrergic fibers may regulate gill vascular tone. Jennings et al. (2004) showed that dorsal aorta and intestinal veins of the eel (*Anguilla australis*) did not contain eNOS, but were innervated with nNOS-positive nerves, and that NO released from this nitrergic fibers regulated smooth muscle vascular tone. Contrary to this, Donald et al. (2004) reported that nNOS-immunoreactive fibers that innervated the dorsal aorta in the shovelnose ray (*Rhinobatus typus*) did not regulate vascular tone. Donald et al. (2004) demonstrated that application of SNP to preconstricted (via acetylcholine) dorsal aortic rings from the ray did not result in relaxation; however application of nicotine did result in aortic ring relaxation. In addition, the nicotine-induced relaxation was not affected by the NOS inhibitor L-NNA or the soluble guanylyl cyclase inhibitor ODQ, suggesting that nicotine-mediated vasodilation was not due to NO production (Donald et al., 2004). These conflicting studies may be the result of species/taxa specific effects. Whether the nitrergic fibers that innervate the gill vasculature in the killifish are involved in regulation of gill vascular tone is undetermined.

4.4. Summary

This was the first study to clone and characterize the complete nNOS sequence from the euryhaline killifish, providing the molecular identity of a signaling enzyme that we previously demonstrated to have an inhibitory role on NaCl secretion (Evans et al., 2004). The killifish nNOS appears to be an orthologue of the mammalian nNOS and shares 75% amino acid similarity with human nNOS. It is expressed at high levels in the gill, opercular epithelium, and kidney of the killifish, tissues that are involved in systemic ion regulation (Karnaky, 1998). Finally, nNOS was immunolocalized to nerve fibers adjacent to blood vessels and epithelial cells neighboring to MRCs in the killifish gill and, therefore, may regulate gill vascular resistance and branchial ion transport as a paracrine signaling molecule.

Acknowledgement

This work was supported by funding from NSF IBN-0089943 and NSF IOB-0519579 to DHE.

References

Alderton, W.K., Cooper, C.E., Knowles, R.G., 2001. Nitric oxide synthases: structure, function and inhibition. Biochem. J. 357, 593–615.

Ando, H., Shi, Q., Kusakabe, T., Ohya, T., Suzuki, N., Urano, A., 2004. Localization of mRNAs encoding alpha and beta subunits of soluble guanylyl cyclase in the brain of rainbow trout: comparison with the distribution of neuronal nitric oxide synthase. Brain Res. 1013, 13–29.

Blaise, G.A., Gauvin, D., Gangal, M., Authier, S., 2005. Nitric oxide, cell signaling and cell death. Toxicology 208, 177–192.

Bordieri, L., Persichini, T., Venturini, G., Cioni, C., 2003. Expression of nitric oxide synthase in the preoptic-hypothalamo-hypophyseal system of the teleost *Oreochromis niloticus*. Brain Behav. Evol. 62, 43–55.

Chenna, R., Sugawara, H., Koike, T., Lopez, R., Gibson, T.J., Higgins, D.G., Thompson, J.D., 2003. Multiple sequence alignment with the Clustal series of programs. Nucleic Acids Res. 31, 3497–3500.

Choe, K.P., Verlander, J.W., Wingo, C.S., Evans, D.H., 2004. A putative H^+-K^+-ATPase in the Atlantic stingray, *Dasyatis sabina*: primary sequence and expression in gills. Am. J. Physiol., Regul. Integr. Comp. Physiol. 287, R981–R991.

Choe, K.P., Kato, A., Hirose, S., Plata, C., Sindic, A., Romero, M.F., Claiborne, J.B., Evans, D.H., 2005. NHE3 in an ancestral vertebrate: primary sequence, distribution, localization, and function in gills. Am. J. Physiol., Regul. Integr. Comp. Physiol. 289, R1520–R1534.

Cioni, C., Bordieri, L., De Vito, L., 2002. Nitric oxide and neuromodulation in the caudal neurosecretory system of teleosts. Comp. Biochem. Physiol., B 132, 57–68.

Crane, B.R., Arvai, A.S., Gachhui, R., Wu, C., Ghosh, D.K., Getzoff, E.D., Stuehr, D.J., Tainer, J.A., 1997. The structure of nitric oxide synthase oxygenase domain and inhibitor complexes. Science 278, 425–431.

Cuoghi, B., Marini, M., Mola, L., 2002. Histochemical and immunocytochemical localization of nitric oxide synthase in the supramedullary neurons of the pufferfish *Tetraodon fluviatilis*. Brain Res. 938, 1–6.

Daff, S., 2003. Calmodulin-dependent regulation of mammalian nitric oxide synthase. Biochem. Soc. Trans. 31, 502–505.

Donald, J.A., Broughton, B.R., Bennett, M.B., 2004. Vasodilator mechanisms in the dorsal aorta of the giant shovelnose ray, *Rhinobatus typus* (Rajiformes; Rhinobatidae). Comp. Biochem. Physiol., A 137, 21–31.

Ebbesson, L.O., Tipsmark, C.K., Holmqvist, B., Nilsen, T., Andersson, E., Stefansson, S.O., Madsen, S.S., 2005. Nitric oxide synthase in the gill of Atlantic salmon: colocalization with and inhibition of Na^+,K^+-ATPase. J. Exp. Biol. 208, 1011–1017.

Evans, D.H., Gunderson, M.P., 1998. A prostaglandin, not NO, mediates endothelium-dependent dilation in ventral aorta of shark (*Squalus acanthias*). Am. J. Physiol., Regul. Integr. Comp. Physiol. 274, R1050–R1057.

Evans, D.H., Harrie, A.C., 2001. Vasoactivity of the ventral aorta of the American eel (*Anguilla rostrata*), Atlantic hagfish (*Myxine glutinosa*), and sea lamprey (*Petromyzon marinus*). J. Exp. Zool. 289, 273–284.

Evans, D.H., Rose, R.E., Roeser, J.M., Stidham, J.D., 2004. NaCl transport across the opercular epithelium of *Fundulus heteroclitus* is inhibited by an endothelin to NO, superoxide, and prostanoid signaling axis. Am. J. Physiol., Regul. Integr. Comp. Physiol. 286, R560–R568.

Evans, D.H., Piermarini, P.M., Choe, K.P., 2005. The multifunctional fish gill: dominant site of gas exchange, osmoregulation, acid–base regulation, and excretion of nitrogenous waste. Physiol. Rev. 85, 97–177.

Farrell, A.P., Johansen, J.A., 1995. Vasoactivity of the coronary artery of rainbow trout, steelhead trout, and dogfish: lack of support for non prostanoid endothelium-derived relaxation factors. Can. J. Zool. 73, 1899–1911.

Felsenstein, J., 2004. PHYLIP (Phylogeny Inference Package) version 3.6. Distributed by the author. Department of Genome Sciences, University of Washington, Seattle.

Fritsche, R., Schwerte, T., Pelster, B., 2000. Nitric oxide and vascular reactivity in developing zebrafish, *Danio rerio*. Am. J. Physiol., Regul. Integr. Comp. Physiol. 279, R2200–R2207.

Funakoshi, K., Kadota, T., Atobe, Y., Nakano, M., Goris, R.C., Kishida, R., 1999. Nitric oxide synthase in the glossopharyngeal and vagal afferent pathway of a teleost, *Takifugu niphobles*. The branchial vascular innervation. Cell Tissue Res. 298, 45–54.

Garcin, E.D., Bruns, C.M., Lloyd, S.J., Hosfield, D.J., Tiso, M., Gachhui, R., Stuehr, D.J., Tainer, J.A., Getzoff, E.D., 2004. Structural basis for isozyme-specific regulation of electron transfer in nitric-oxide synthase. J. Biol. Chem. 279, 37918–37927.

Gibbins, I.L., Olsson, C., Holmgren, S., 1995. Distribution of neurons reactive for NADPH-diaphorase in the branchial nerves of a teleost fish, *Gadus morhua*. Neurosci. Lett. 193, 113–116.

Guindon, S., Lethiec, F., Duroux, P., Gascuel, O., 2005. PHYML Online—a web server for fast maximum likelihood-based phylogenetic inference. Nucleic Acids Res. 33, W557–W559.

Hoffmann, E.K., Hoffmann, E., Lang, F., Zadunaisky, J.A., 2002. Control of Cl (−) transport in the operculum epithelium of *Fundulus heteroclitus*: long- and short-term salinity adaptation. Biochim. Biophys. Acta 1566, 129–139.

Holmqvist, B., Ellingsen, B., Alm, P., Forsell, J., Oyan, A.M., Goksoyr, A., Fjose, A., Seo, H.C., 2000. Identification and distribution of nitric oxide synthase in the brain of adult zebrafish. Neurosci. Lett. 292, 119–122.

Ignarro, L.J., Buga, G.M., Wood, K.S., Byrns, R.E., Chaudhuri, G., 1987. Endothelium-derived relaxing factor produced and released from artery and vein is nitric oxide. Proc. Natl. Acad. Sci. U. S. A. 84, 9265–9269.

Jennings, B.L., Broughton, B.R., Donald, J.A., 2004. Nitric oxide control of the dorsal aorta and the intestinal vein of the Australian short-finned eel *Anguilla australis*. J. Exp. Biol. 207, 1295–1303.

Jonz, M.G., Nurse, C.A., 2003. Neuroepithelial cells and associated innervation of the zebrafish gill: a confocal immunofluorescence study. J. Comp. Neurol. 461, 1–17.

Karnaky Jr., K.J., 1998. Osmotic and ionic regulation. In: Evans, D.H. (Ed.), The Physiology of Fishes. CRC Press LLC, New York, pp. 157–176.

Karnaky Jr., K.J., Kinter, W.B., 1977. Killifish opercular skin: a flat epithelium with a high density of chloride cells. J. Exp. Zool. 199, 355–364.

Karnaky Jr., K.J., Kinter, L.B., Kinter, W.B., Stirling, C.E., 1976. Teleost chloride cell: II. Autoradiographic localization of gill Na,K-ATPase in killifish *Fundulus heteroclitus* adapted to low and high salinity environments. J. Cell Biol. 70, 157–177.

Katoh, F., Hasegawa, S., Kita, J., Takagi, Y., Kaneko, T., 2001. Distinct seawater and freshwater types of chloride cells in killifish, *Fundulus heteroclitus*. Can. J. Zool. 79, 822–829.

Katoh, F., Hyodo, S., Kaneko, T., 2003. Vacuolar-type proton pump in the basolateral plasma membrane energizes ion uptake in branchial mitochondria-rich cells of killifish *Fundulus heteroclitus*, adapted to a low ion environment. J. Exp. Biol. 206, 793–803.

Laemmli, U.K., 1970. Cleavage of structural proteins during the assembly of the head of bacteriophage T4. Nature 227, 680.

Marshall, W.S., Emberley, T.R., Singer, T.D., Bryson, S.E., McCormick, S.D., 1999. Time course of salinity adaptation in a strongly euryhaline estuarine teleost, *Fundulus heteroclitus*: a multivariable approach. J. Exp. Biol. 202, 1535–1544.

Masters, B.S., McMillan, K., Sheta, E.A., Nishimura, J.S., Roman, L.J., Martasek, P., 1996. Neuronal nitric oxide synthase, a modular enzyme formed by convergent evolution: structure studies of a cysteine thiolate-liganded heme protein that hydroxylates L-arginine to produce NO as a cellular signal. FASEB J. 10, 552–558.

Mauceri, A., Fasulo, S., Ainis, L., Licata, A., Lauriano, E.R., Martinez, A., Mayer, B., Zaccone, G., 1999. Neuronal nitric oxide synthase (nNOS) expression in the epithelial neuroendocrine cell system and nerve fibers in the gill of the catfish, *Heteropneustes fossilis*. Acta Histochem. 101, 437–448.

McGeer, J.C., Eddy, F.B., 1996. Effects of sodium nitroprusside on blood circulation and acid–base and ionic balance in rainbow trout: Indications for nitric oxide induced vasodilation. Can. J. Zool. 74, 1211–1219.

McMillan, K., Masters, B.S., 1995. Prokaryotic expression of the heme- and flavin-binding domains of rat neuronal nitric oxide synthase as distinct polypeptides: identification of the heme-binding proximal thiolate ligand as cysteine-415. Biochemistry 34, 3686–3693.

Olson, K.R., Villa, J., 1991. Evidence against nonprostanoid endothelium-derived relaxing factor(s) in trout vessels. Am. J. Physiol., Regul. Integr. Comp. Physiol. 260, R925–R933.

Olson, K.R., Conklin, D.J., Farrell, A.P., Keen, J.E., Takei, Y., Weaver, L., Smith, M.P., Zhang, Y.T., 1997. Effects of natriuretic peptides and nitroprusside on venous function in trout. Am. J. Physiol., Regul. Integr. Comp. Physiol. 273, R527–R539.

Oyan, A.M., Nilsen, F., Goksoyr, A., Holmqvist, B., 2000. Partial cloning of constitutive and inducible nitric oxide synthases and detailed neuronal expression of NOS mRNA in the cerebellum and optic tectum of adult Atlantic salmon (*Salmo salar*). Brain Res. Mol. Brain Res. 78, 38–49.

Palmer, R.M.J., Ferrige, A.G., Moncada, S., 1987. Nitric-oxide release accounts for the biological-activity of endothelium-derived relaxing factor. Nature 327, 524–526.

Piermarini, P.M., Verlander, J.W., Royaux, I.E., Evans, D.H., 2002. Pendrin immunoreactivity in the gill epithelium of a euryhaline elasmobranch. Am. J. Physiol., Regul. Integr. Comp. Physiol. 283, R983–R992.

Rose, T.M., Henikoff, J.G., Henikoff, S., 2003. CODEHOP (COnsensus-DEgenerate Hybrid Oligonucleotide Primer) PCR primer design. Nucleic Acids Res. 31, 3763–3766.

Soderstrom, V., Hylland, P., Nilsson, G.E., 1995. Nitric oxide synthase inhibitor blocks acetylcholine induced increase in brain blood flow in rainbow trout. Neurosci. Lett. 197, 191–194.

Tipsmark, C.K., Madsen, S.S., 2003. Regulation of Na^+/K^+-ATPase activity by nitric oxide in the kidney and gill of the brown trout (*Salmo trutta*). J. Exp. Biol. 206, 1503–1510.

Tota, B., Amelio, D., Pellegrino, D., Ip, Y.K., Cerra, M.C., 2005. NO modulation of myocardial performance in fish hearts. Comp. Biochem. Physiol., A 142, 164–177.

Zaccone, G., Ainis, L., Mauceri, A., Lo Cascio, P., Lo Giudice, F., Fasulo, S., 2003. NANC nerves in the respiratory air sac and branchial vasculature of the Indian catfish, *Heteropneustes fossilis*. Acta Histochem. 105, 151–163.

Zhang, J., Martasek, P., Paschke, R., Shea, T., Siler Masters, B.S., Kim, J.J., 2001. Crystal structure of the FAD/NADPH-binding domain of rat neuronal nitric-oxide synthase. Comparisons with NADPH-cytochrome P450 oxidoreductase. J. Biol. Chem. 276, 37506–37513.